Supplementary Information (SI) for Chemical Communications.

SUPPORTING INFORMATIONS

Photomodulation of dinuclear europium(III) complexes luminescence using thermally reversible photochromism of diarylethene

Yoann Fréroux,[a] Salauat Kiraev,[b] Olivier Galangau,[a] Tuan-Anh Phan,[a] Thierry Roisnel,[a] Olivier Maury,[b] Stéphane Rigaut [a] and Lucie Norel *,[a,c]

Table of contents

1. General comments

Reactions were carried out under an Argon atmosphere using Schlenk techniques. Dichloromethane was taken from MB SPS-800 machine. Reagents were purchased from ACROS Organics and from ALDRICH Chemical Co. ^{1}H NMR ^{13}C NMR, ^{19}F NMR spectra were recorded using Bruker Advance 400 (400 MHz), or 500 (500 MHz) spectrometers. Note that for some paramagnetic lanthanide complexes, it was not possible to assign all of the signals precisely as well as to obtain ^{13}C and 2D NMR.

Elemental analyses and high-resolution mass spectrometry were performed at Centre Régional de Mesures Physiques de l’Ouest.

2. Synthetic Procedures

Synthesis of **1Eu$_o$**:

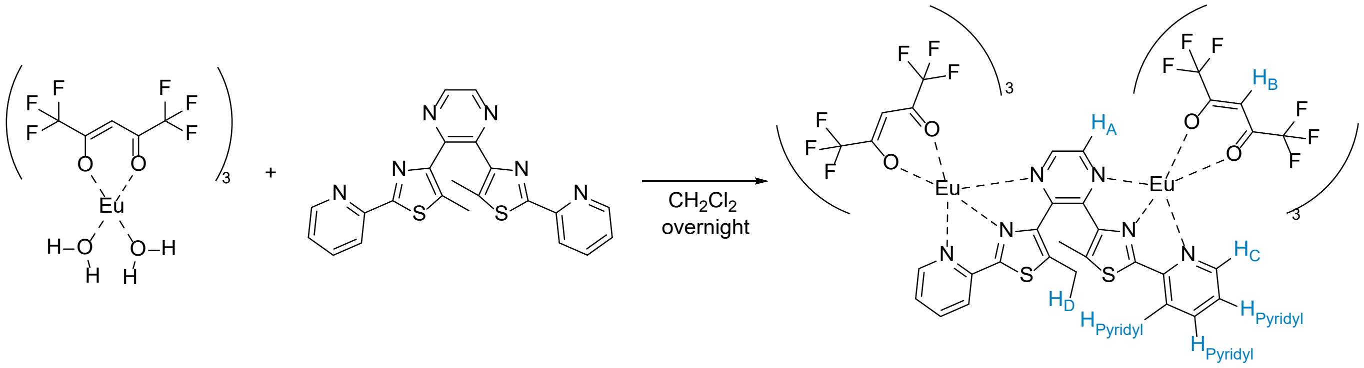

2,3-bis(5-methyl-2-(pyridine-2-yl)thiazol-4-yl)pyrazine[1] (21.4 mg, 0.05 mmol, 1 eq.) and [Eu(hfac)$_3$.2H$_2$O)] (82.9 mg, 0.10 mmol, 2.05 eq.) were mixed in 4 mL of dichloromethane and the mixture was refluxed for 15 min to observe complete solubilization. Upon slow cooling, block shaped crystals were obtained. A second crop of similar crystals was obtained after cooling at -20°C. The total yield was 52 mg (0.07 mmol, 50 %).

^{1}H NMR (400 MHz, CD$_2$Cl$_2$): δ (ppm) = 44.24 (s, 2H, H$_A$), 40.39 (s, 2H, H$_C$), 14.38 (s, 2H, H$_{Pyridyl}$), 11.14 (s, 1H, H$_{Pyridylr}$), 7.19 (s, 2H, H$_{Pyridyl}$), 1.69 (s, 6H, H$_B$), -1.80 (s, 6H, H$_D$).

^{13}C NMR (101 MHz, CD$_2$Cl$_2$): δ (ppm) = 155.64, 151.82, 143.67, 125.01, 119.69, 102.66, 97.18, 55.81, 10.25.

^{19}F{H} NMR (376 MHz, CD$_2$Cl$_2$) δ (ppm) = -80.33 (s, 36F, CF$_3$).

HR-MS ESI (CHCl$_3$): *m/z* calcd for [C_{47} H_{21} N_6 O_{10} F_{30} S_2 Eu_2]$^+$ [M - hfac]$^+$: 1767.870434 ,: Found : 1767.870387 (1 ppm) [M - hfac]$^+$.

Elem. Anal. Calcd for C_{52} H_{22} N_6 O_{12} F_{36} S_2 Eu_2 : C, 31.63; H, 1.12; N, 4.26; S, 3.25 Found: C, 31.99; H, 1.04; N, 4.20; S, 3.08

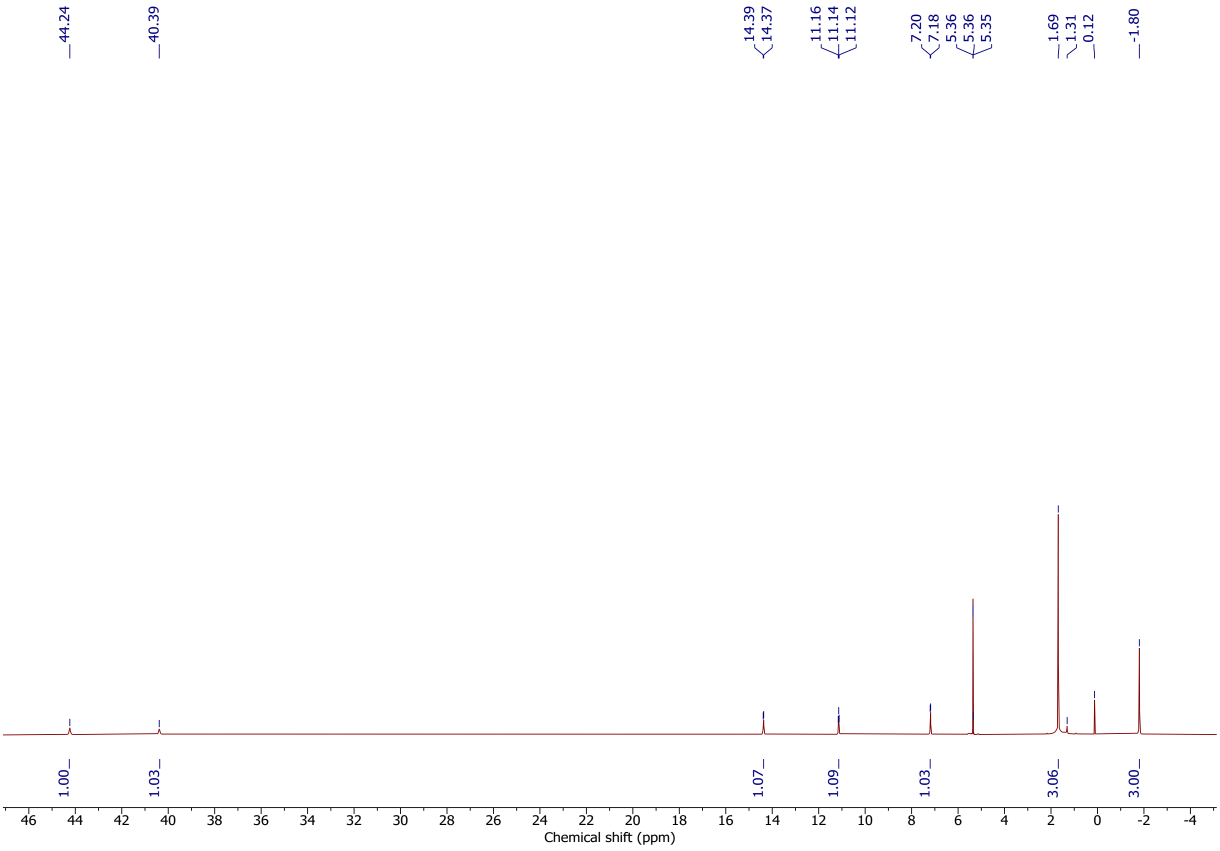

Figure S1: ^{1}H (400 MHz, CD_2Cl_2) NMR spectrum of **1Eu$_o$**, C ~10^{-3}M.

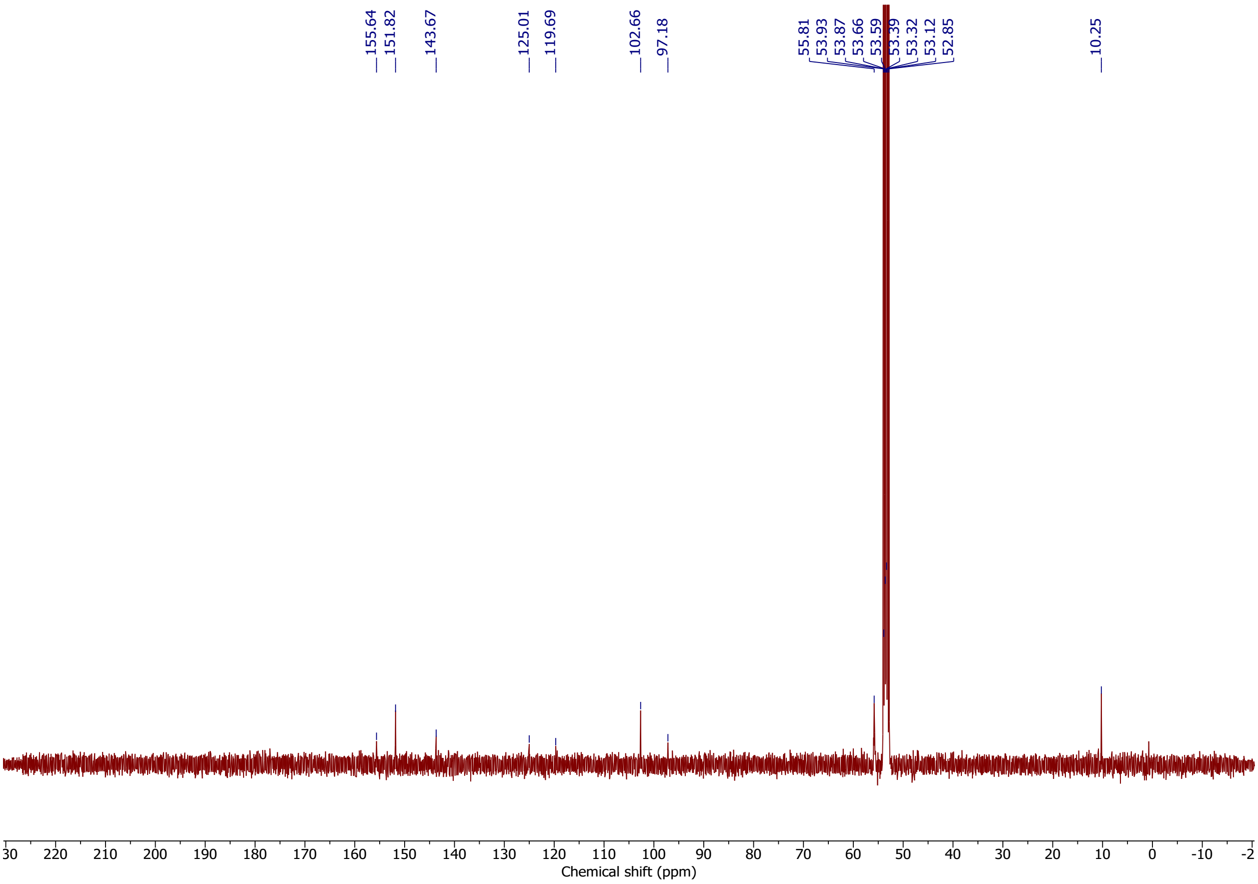

Figure S2: $^{13}C\{^1H\}$ (101 MHz, CD_2Cl_2) NMR spectrum of **1Eu$_o$**, C ~10^{-3}M.

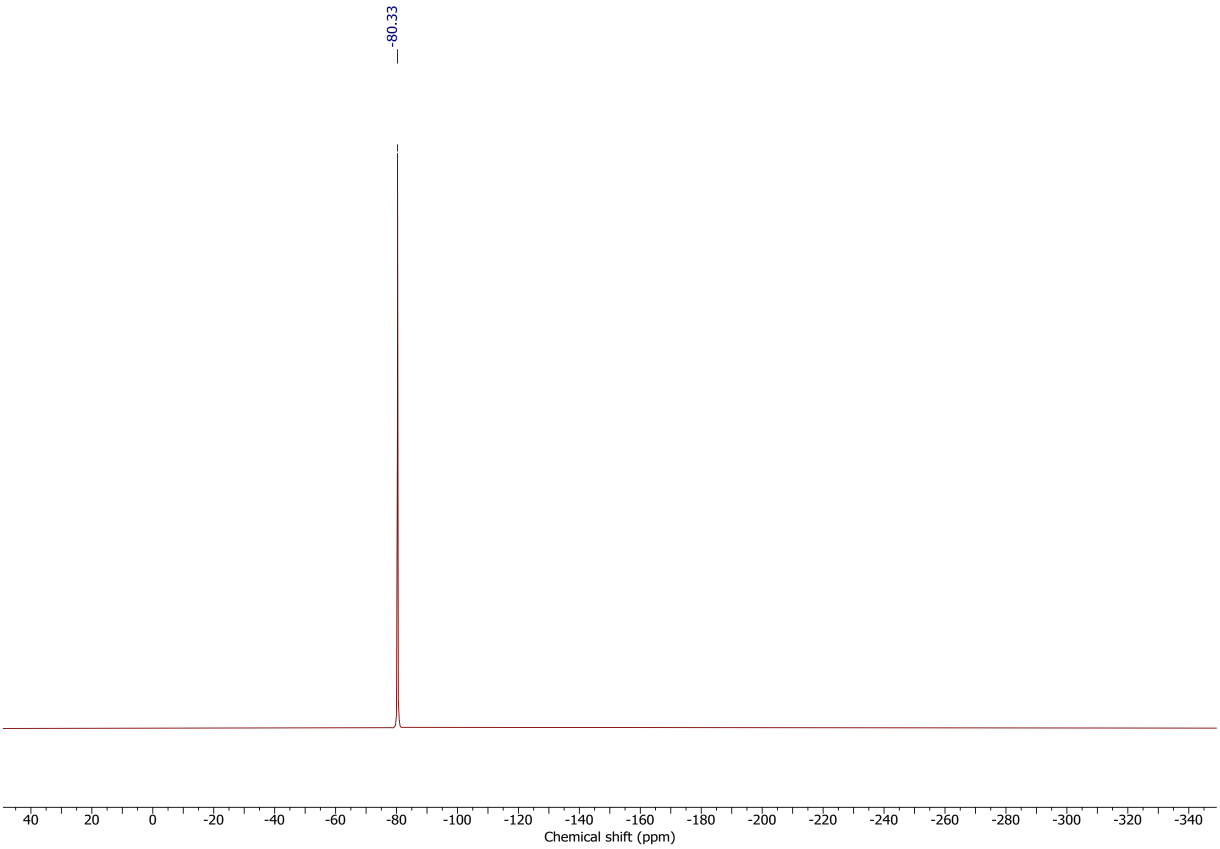

Figure S3: $^{19}F\ \{^1H\}$ (376 MHz, CD_2Cl_2) NMR spectrum of **1Eu**$_o$, C ~10^{-3}M.

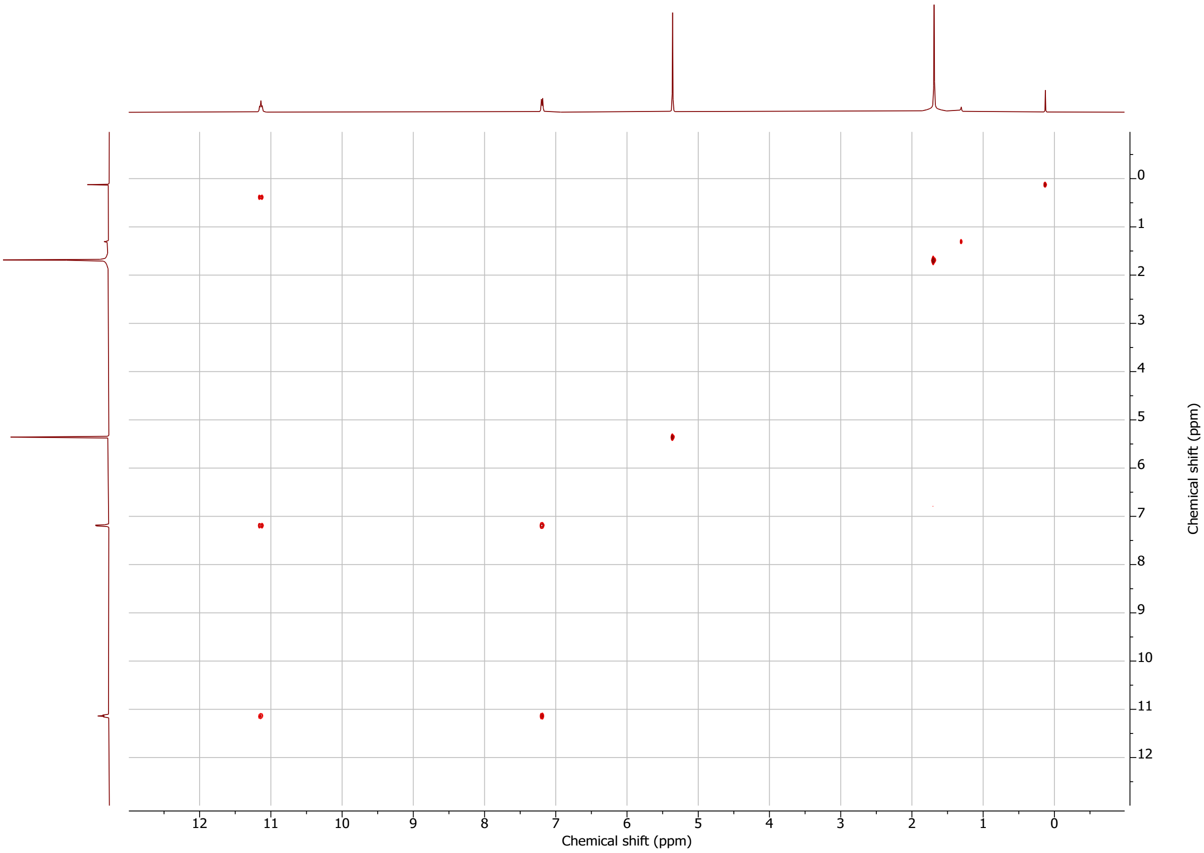

Figure S4: COSY NMR spectrum of **1Eu**$_o$, C ~10^{-3}M.

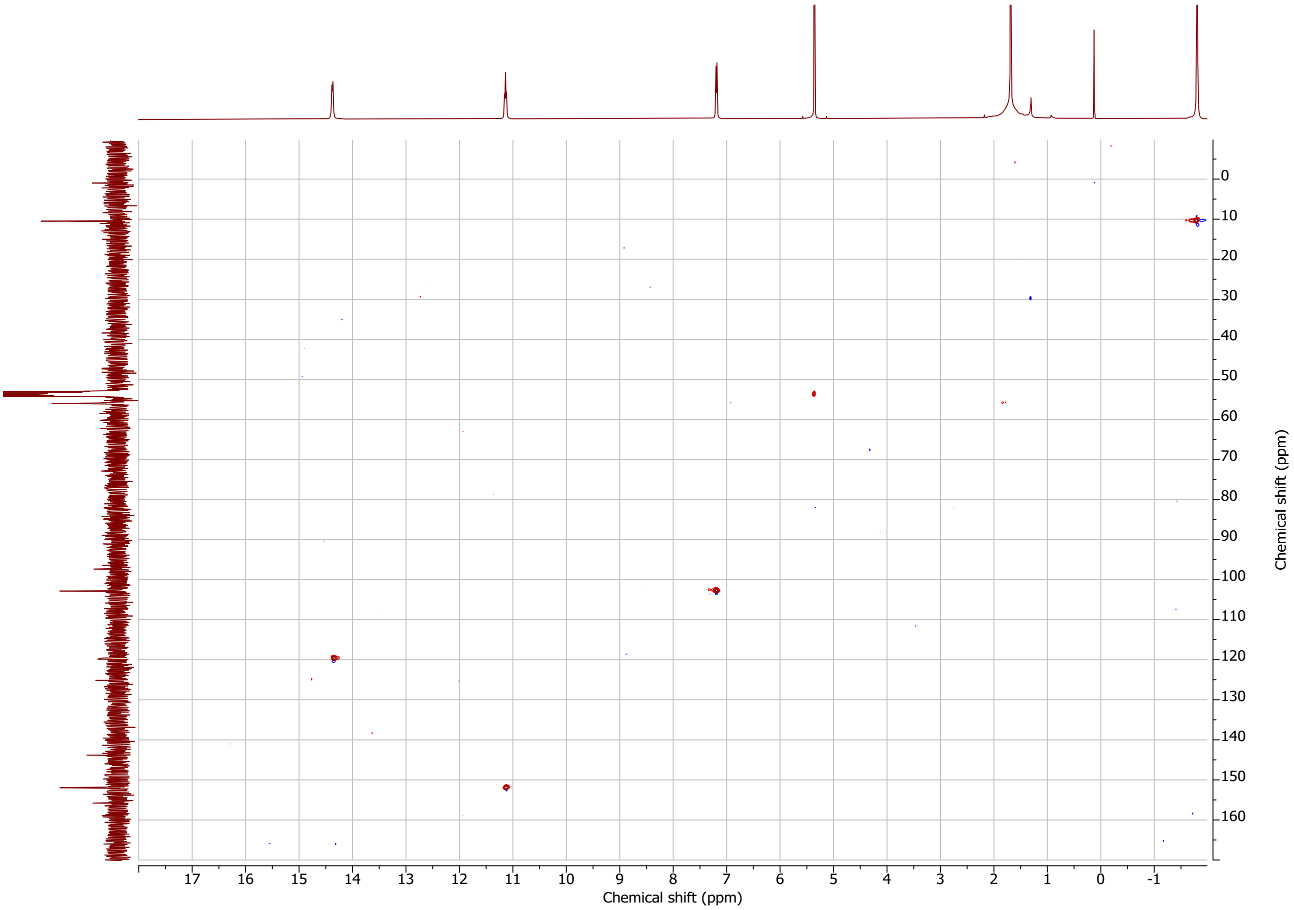

Figure S5: HSQC NMR spectrum of **1Euₒ**, C ~10^{-3}M.

Synthesis of **1Yb**$_{o}$:

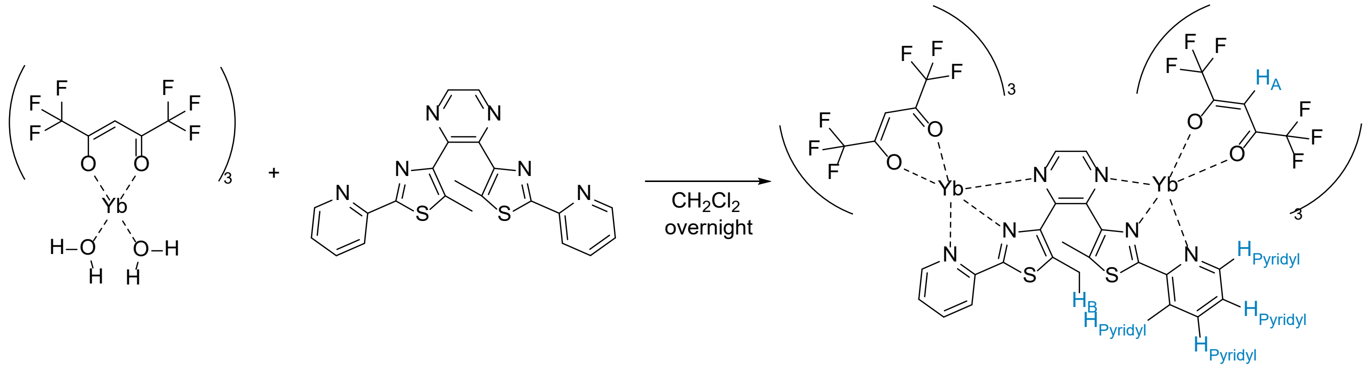

2,3-bis(5-methyl-2-(pyridine-2-yl)thiazol-4-yl)pyrazine[1] (45 mg, 0.15 mmol, 1 eq.) and [Yb(hfac)$_3$.2H$_2$O)] (173 mg, 0.31 mmol, 2.05 eq.) were mixed in 4 mL of dichloromethane and the mixture was refluxed for 15 min to observe complete solubilization. Upon slow cooling, block shaped crystals were obtained. A second crop of similar crystals was obtained after cooling at -20°C. The total yield was 103 mg (0.07 mmol, 53 %).

^{1}H NMR (500 MHz, CD$_2$Cl$_2$): *δ* (ppm) = 42.82 (bs, 2H, H$_{Pyridyl}$), 22.72 (bs, 2H, H$_{Pyridyl}$), 10.77 (s, 2H, H$_{Pyridyl}$), 1.30 (bs, 6H, H$_B$), -15.24 (bs, 6H, H$_A$). Note that protons in ortho positions on the heterocycles are not observed due to severe paramagnetic shifts and relaxation enhancement.

^{19}F{H} NMR (376 MHz, CD$_2$Cl$_2$) δ (ppm) = -85.31 (s, 36F, F$_{hfac}$).

HR-MS ESI (CHCl$_3$): *m/z* calcd for [C$_{47}$ H$_{21}$ N$_6$ O$_{10}$ F$_{30}$ S$_2$ Yb$_2$]$^+$ [M - hfac]$^+$: 1810.90535 ,Found : 1810.9056 (0 ppm) [M - hfac]$^+$.

Elem. Anal. Calcd for C$_{52}$ H$_{22}$ N$_6$ O$_{12}$ F$_{36}$ S$_2$ Yb$_2$: C, 30.97; H, 1.10; N, 4.17; S, 3.18, Found: C, 30.76; H, 1.25; N, 4.08; S, 3.62

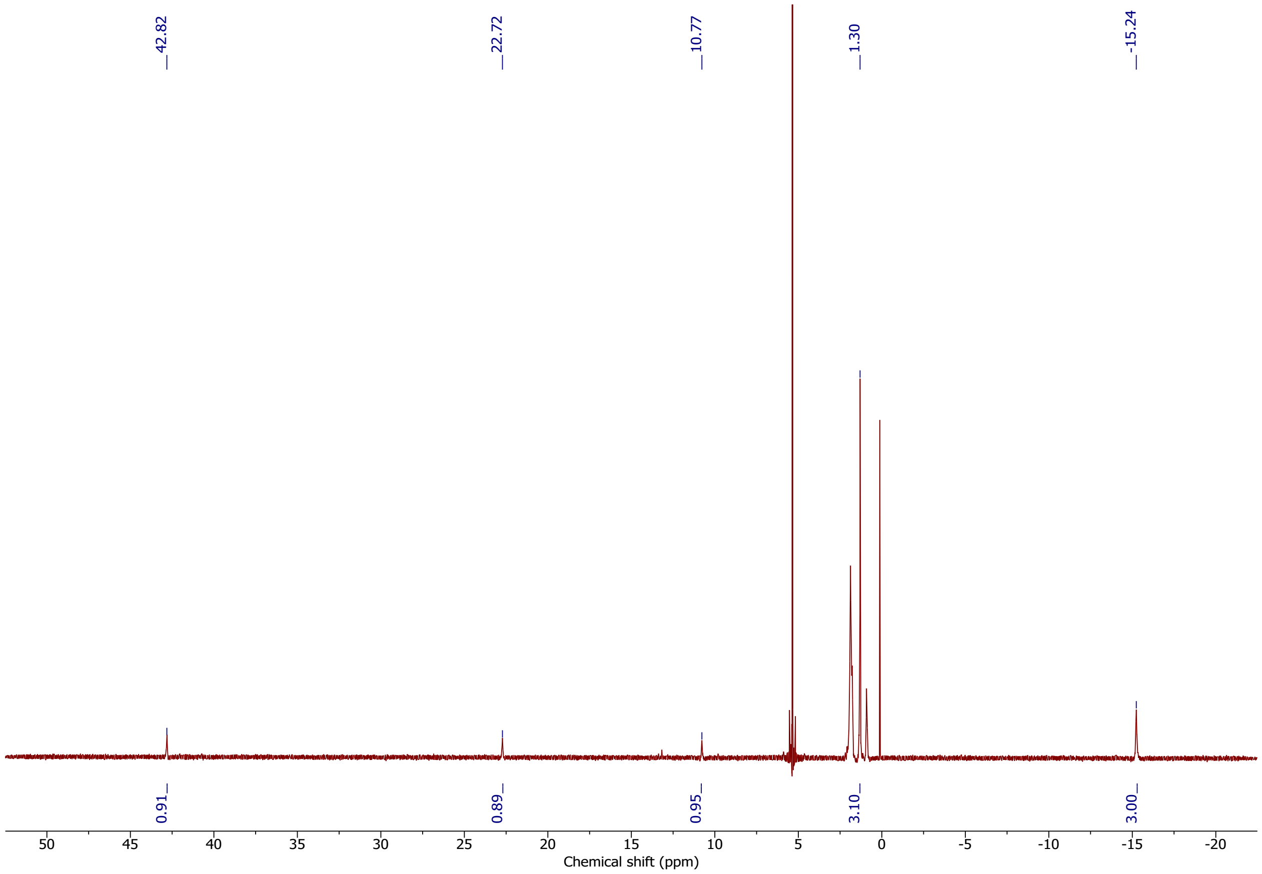

Figure S6: ^{1}H (500 MHz, CD_2Cl_2) NMR spectrum of **$1Yb_o$**, C >10^{-3}M.

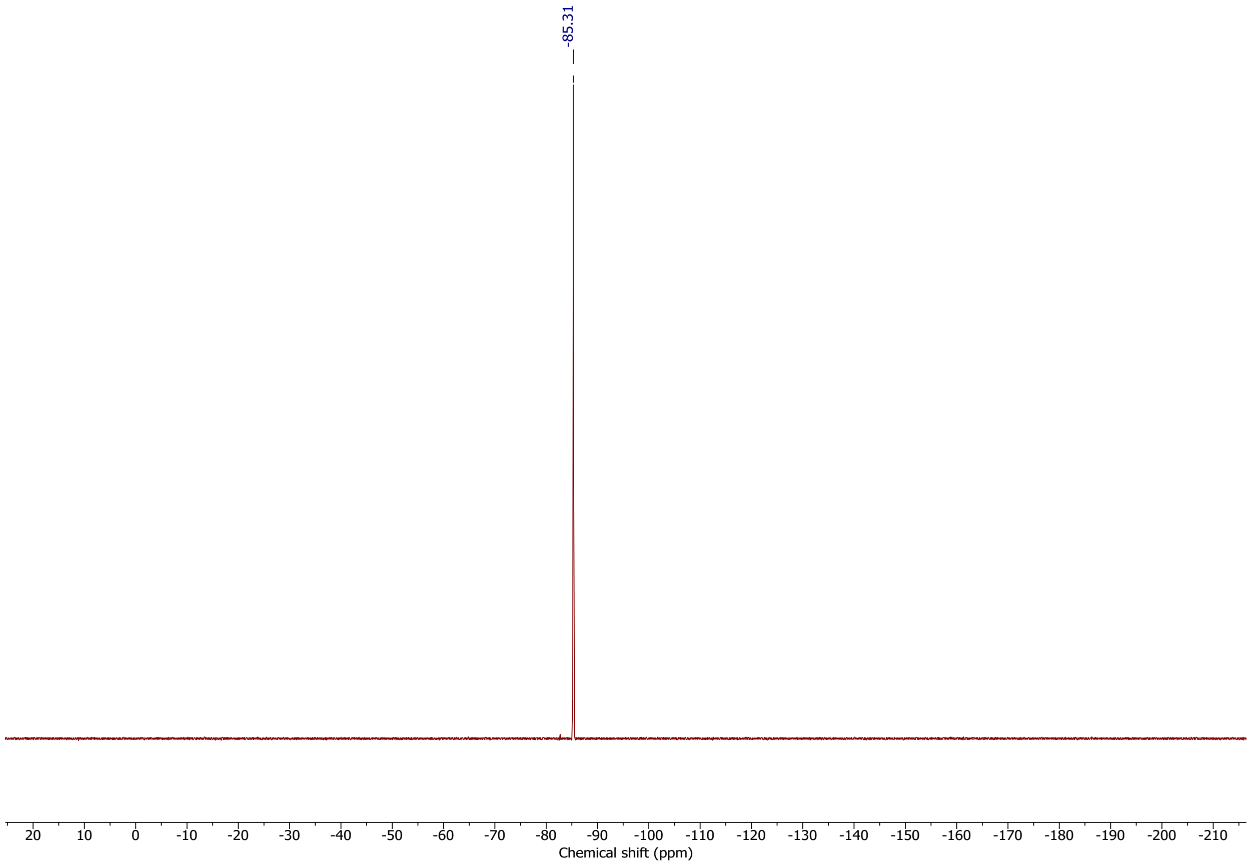

Figure S7: ^{19}F {^{1}H} (376 MHz, CD_2Cl_2) NMR spectrum of **$1Yb_o$**, C >10^{-3}M.

3. NMR Titration and dilution experiments

In order to estimate the coordination behavior of the DAE with Yb, compound **BTP$_o$** was fetched in an NMR tube ([c] ~ 2×10^{-3} mol.L^{-1}) and a deuterated solution of **Yb(hfac)$_3$** is progressively added (from 0.5 to 7 equivalent) into the NMR tube. Upon following ^{1}H NMR spectrum, three different species are observed, the initial ligand **BTP$_o$**, the 1:1 coordinated intermediate (yellow highlighted signals) and the 2:1 coordinated product **1Yb$_o$**. The titration is stopped when the stoichiometry is well exceeded (7 equivalents instead of the 2 equivalents expected) and no more evolution takes place.

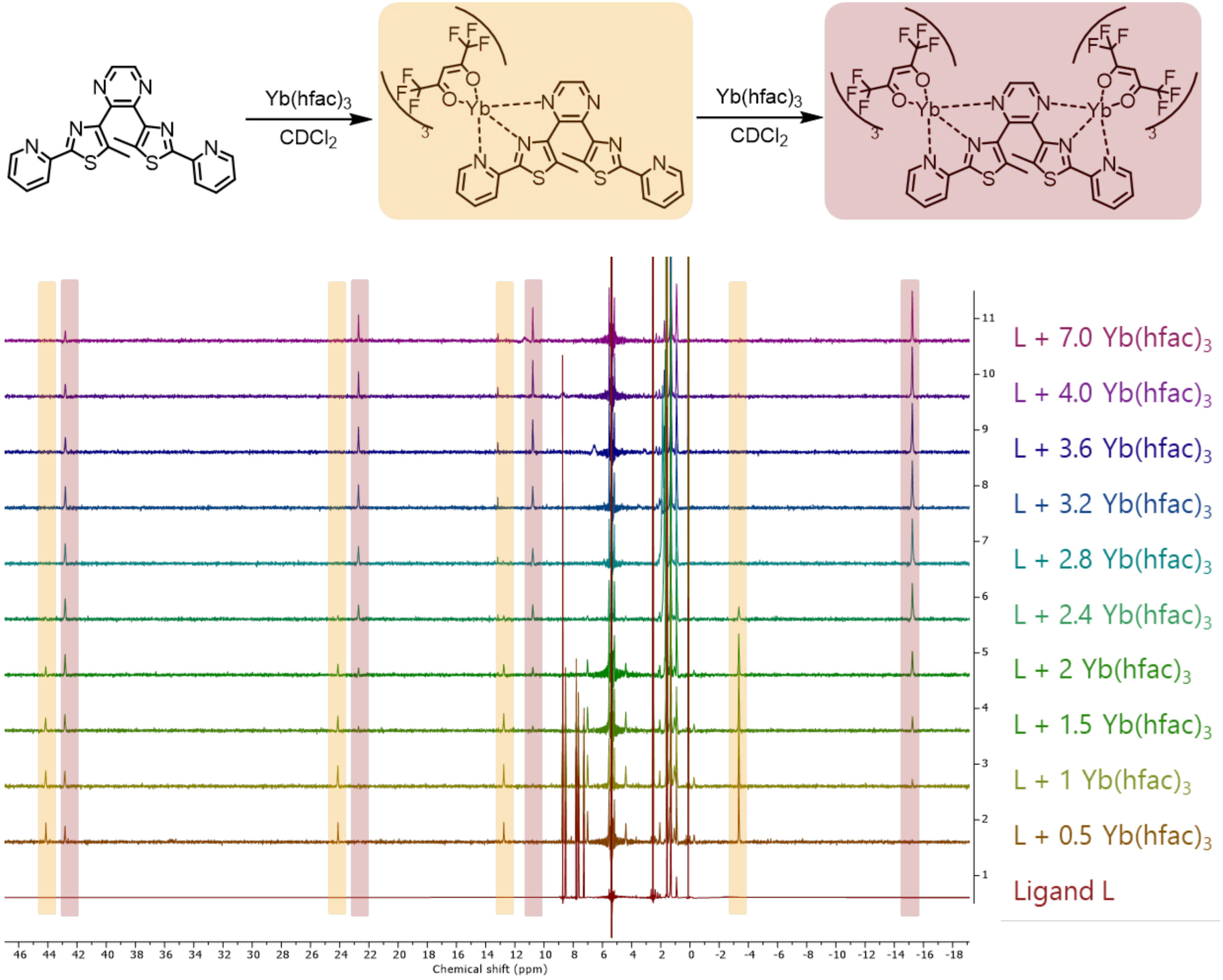

Figure S8: ^{1}H (500 MHz, CD$_2$Cl$_2$, 298 K) NMR titration of BTP$_o$ by Yb(hfac)$_3$ (3,84 × 10^{-4} M ≤ [BTP$_o$] ≤ 3.27× 10^{-3} M and 0 M ≤ [Yb(hfac)$_3$] ≤ 3.27× 10^{-3} M).

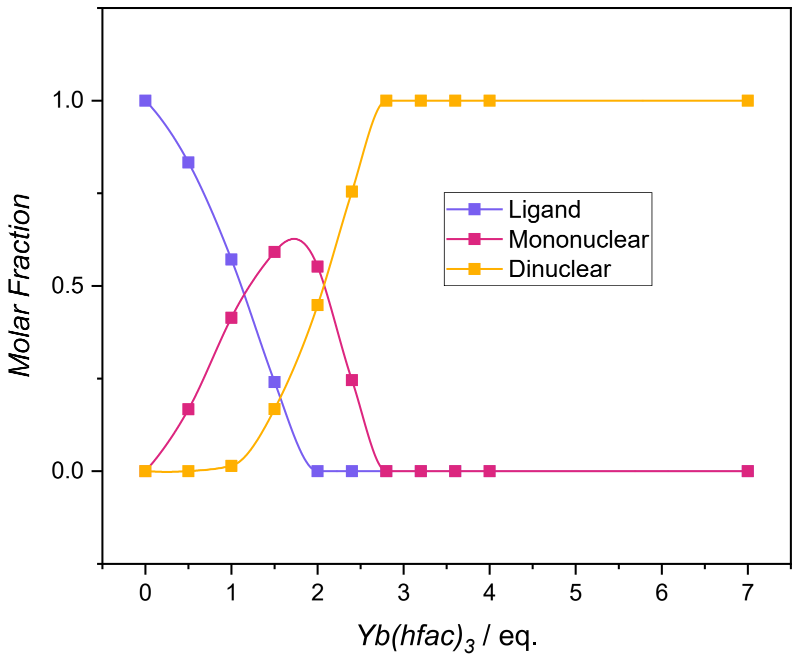

Figure S9: Composition of the mixture of initial ligand, intermediate mononuclear and final dinuclear product **1Yb$_o$** deduced by integration of ^{1}H NMR titration of BTP$_o$ by Yb(hfac)$_3$ in CD$_2$Cl$_2$ at 298 K (3,84 × 10^{-4} M ≤ [BTP$_o$] ≤ 3.27× 10^{-3} M and 0 M ≤ [Yb(hfac)$_3$] ≤ 3.27× 10^{-3} M). Lines are guide to the eye.

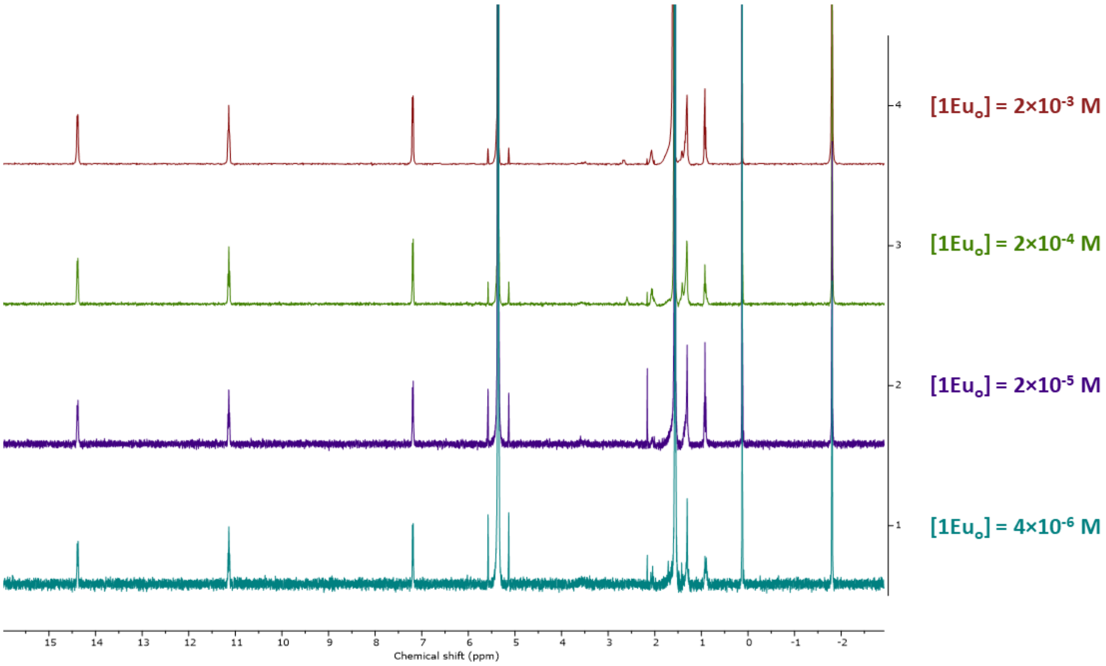

Figure S10: ^{1}H (400 MHz, CD$_2$Cl$_2$, 298 K) NMR dilution of **1Eu$_o$** (2.0 × 10^{-3} M ≤ [**1Eu$_o$**] ≤ 4.0 × 10^{-6} M, 64 to 2048 scans, respectively).

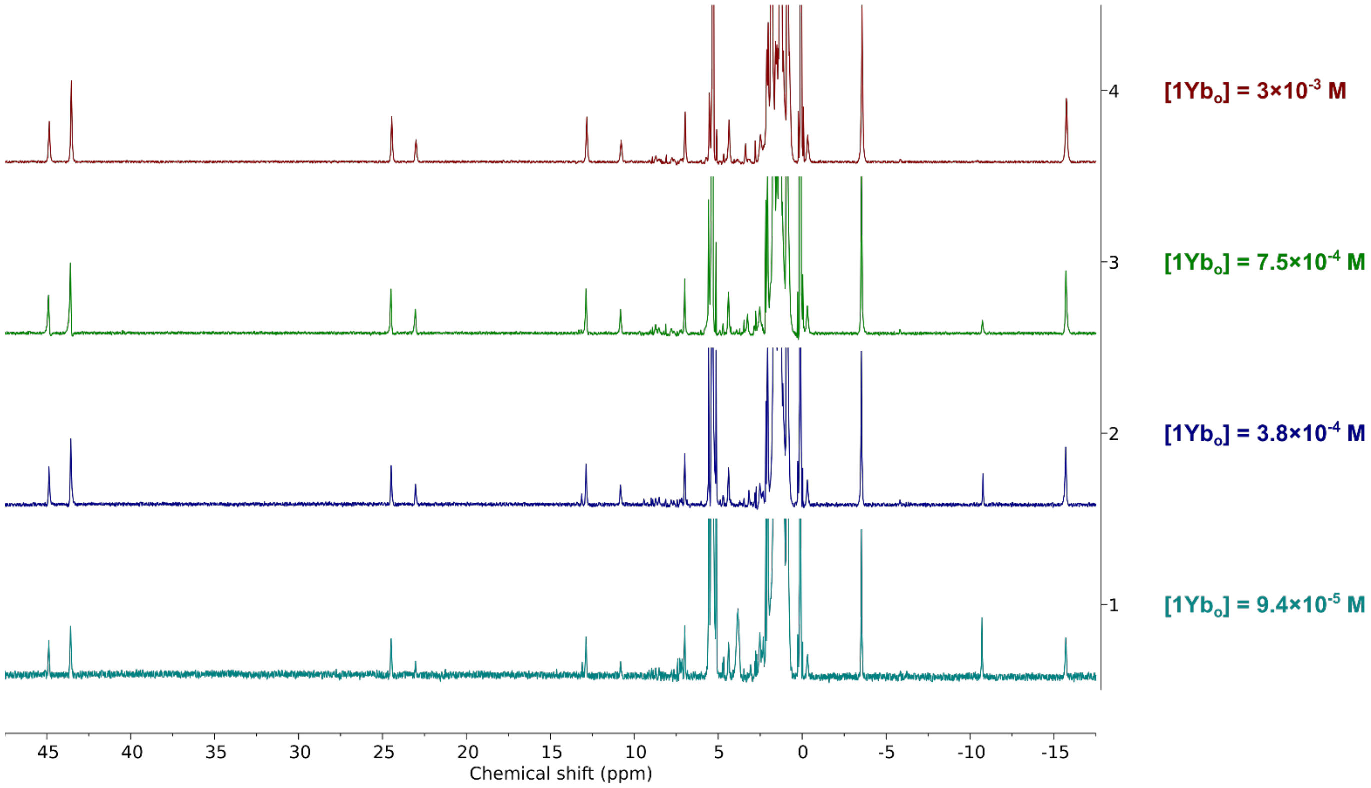

Figure S11: ^{1}H (400 MHz, CD_2Cl_2, 298 K) NMR dilution of **1Yb$_o$** (3.0×10^{-3} M ≤ [**1Yb$_o$**] ≤ 9.4×10^{-5} M, 32 to 256 scans, respectively).

4. Crystallographic Studies

X-Ray measurements were performed at 150(2) K with a crystal mounted with a cryoloop on the goniometer head of a D8 Venture Bruker AXS diffractometer (multilayer monochromator, Mo Kα radiation, λ = 0.710 73 Å). The structure was solved by dual-space algorithm using the SHELXT program, and then refined with full-matrix least-squares methods based on F2 (SHELXL). All non-hydrogen atoms were refined with anisotropic atomic displacement parameters. H atoms were finally included in their calculated positions and treated as riding on their parent atom with constrained thermal parameters. These data can be obtained free of charge from The Cambridge Crystallographic Data Centre via www.ccdc.cam.ac.uk/data_request/cif.].

	1Eu$_o$
Formula	$C_{52}H_{22}Eu_2F_{36}N_6O_{12}S_2$
FW	1974.79
Cryst. Syst.	Monoclinic
Space group	C 2/c
a (Å)	15.0598 (15)
b (Å)	22.670 (2)
c (Å)	19.377 (2)
α (Å)	90
β (Å)	92.999 (4)
γ (Å)	90
V (Å^{3})	6606.5 (12)
Z	4
D_{ca} (g.cm^{-3})	1.985
T (K)	150(2)
Final R (I> 2σ)	0.0221
R_w (all)	0.0680

Table S1: Crystal data and structure refinement parameters for ***1Eu$_o$****.*

Bond	**Bond length**
Eu1-O51	2.3741(15)
Eu1-O55	2.3868(16)
Eu1-O21	2.4002(16)
Eu1-O1	2.4225(16)
Eu1-O25	2.4308(16)
Eu1-O5	2.4361(15)
Eu1-N78	2.5169(17)
Eu1-N71	2.6343(18)
Eu1-N83	2.6691(17)

Table S2: Selected bond lengths from ***1Eu$_o$***

	$1Yb_o$
Formula	$C_{52}H_{22}Yb_2F_{36}N_6O_{12}S_2$
FW	2016.95
Cryst. Syst.	Monoclinic
Space group	$P\ 2_1/n$
a (Å)	12.4171 (7)
b (Å)	32.1311 (19)
c (Å)	18.2736 (11)
α (Å)	90
β (Å)	105.030 (2)
γ (Å)	90
V ($Å^3$)	7041.3 (7)
Z	4
D_{ca} ($g.cm^{-3}$)	1.903
T (K)	150(2)
Final R (I> 2σ)	0.0350
R_w (all)	0.0864

*Table S3: Crystal data and structure refinement parameters for **$1Yb_o$***

Bond	**Bond length**	**Bond**	**Bond length**
Yb1-O22	2.295(3)	Yb2-O101	2.284(3)
Yb1-O21	2.297(3)	Yb2-O121	2.290(3)
Yb1-O41	2.339(3)	Yb2-O145	2.290(3)
Yb1-O5	2.348(3)	Yb2-O141	2.298(3)
Yb1-O45	2.362(3)	Yb2-O125	2.303(3)
Yb1-O1	2.366(3)	Yb2-O105	2.313(3)
Yb1-N68	2.426(3)	Yb2-N168	2.466(3)
Yb1-N61	2.542(3)	Yb2-N161	2.532(3)
Yb1-N73	2.581(3)		

*Table S4: Selected bond lengths from **$1Yb_o$***

5. Photophysical studies

Electronic Absorption measurements were performed in dichloromethane solutions at room temperature using “UV VIS NIR JASCO” spectrometer.

Molar extinction coefficient values were measured following Beer’s law:

$$\epsilon = \frac{A}{CL}$$

where A is the absorbance, C is the concentration and L is the length of the optical path. In each case, two set of ten diluted solutions are measured in order to obtain to slope corresponding to the ε values. The percentage of difference between the two ε values give a experimental uncertainty value “δ" leading to the following molar extinction value: $\varepsilon \pm \delta$ $M^{-1}.cm^{-1}$.

The luminescence measurements were performed using Horiba-Jobin Yvon Fluorolog-3® spectrofluorimeters. The steady-state luminescence was excited by a 450 W Xenon CW lamp and detected at an angle of 90° with either a Hamamatsu R928 photomultiplier tube for the visible range (single grating emission monochromator with dispersions of 2.1 nm/mm (1200 grooves per mm)) or a liquid nitrogen cooled Symphony® II CCD detector for the full and instantaneous spectral acquisition in the near infrared range (single grating with a dispersion of 4.9 nm/mm (600 or 150 grooves/mm)) and the InGaAs detector for the anti-photobleaching mode in the near infrared range. Spectra were reference corrected for both the excitation source light intensity variation (lamp and grating) and the emission spectral response (detectors and gratings).

The sample were dissolved in dichloromethane and placed either in 1 cm squared cuvettes measurements at RT or 4 mm width quartz tubes inserted in a quartz Dewar filled with liquid nitrogen for 77 K measurements. To measure luminescence quenching, we limited the volume of the solution in the cuvette to the strict minimum (1 mL) so that the whole solution was illuminated. To measure the thermal return, the anti-photobleaching mode (UV Off) of the spectrometer was used successively after auto shutter control (UV On). The UG-11 (280–380 nm) band-pass filter was placed before the cuvette for each experiment to avoid the second order scatter.

	λ_{abs} (nm)	λ_{em} (nm)	ε ($M^{-1}.cm^{-1}$)
$1Yb_o$	305	975	81 000
$1Eu_o$	309	615	84 000

Table S5: Photophysical properties of the studied compounds

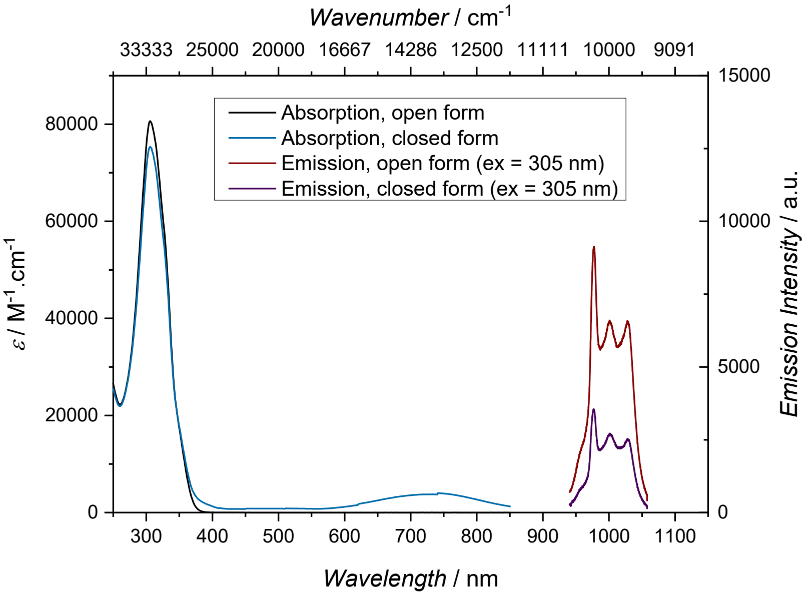

Figure S12: Electronic absorption and emission (λ_{ex} = 305 nm) spectrum of **$1Yb_o$** and the photostationary state upon photoisomerization (λ_{ex} = 365nm), dichloromethane, 20°C, C = 4.4 10^{-6} M. The complex is partially dissociated at this concentration.

.

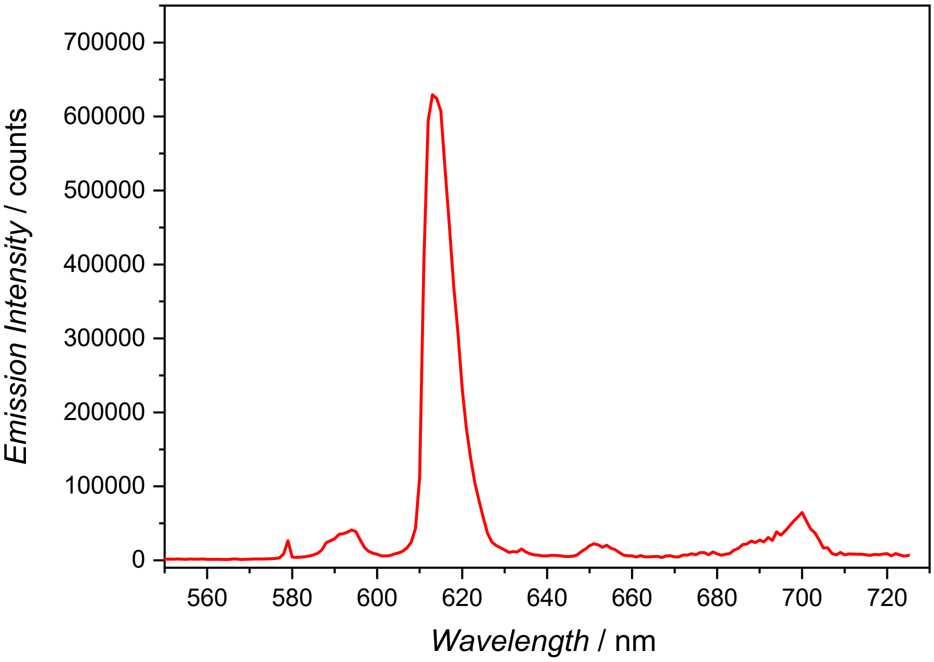

Figure S13: Emission spectrum of **1Eu$_o$** at λ_{ex} = 350 nm in dichloromethane, RT, C = 1.5 10^{-6} M.

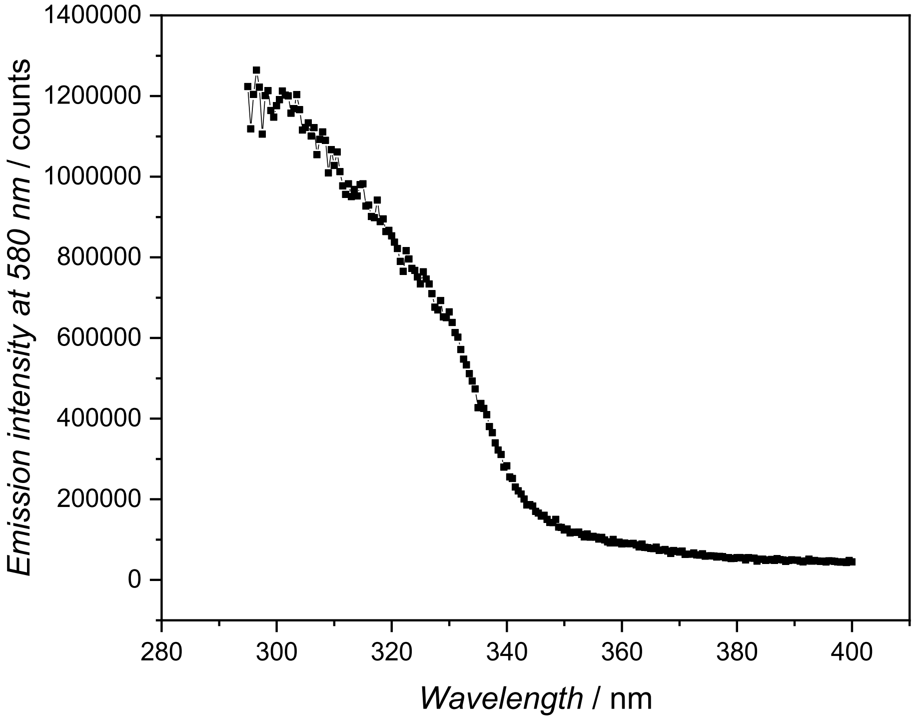

Figure S14: Excitation spectrum of **1Eu$_o$** in dichloromethane, RT, C = 1.5 10^{-6} M.

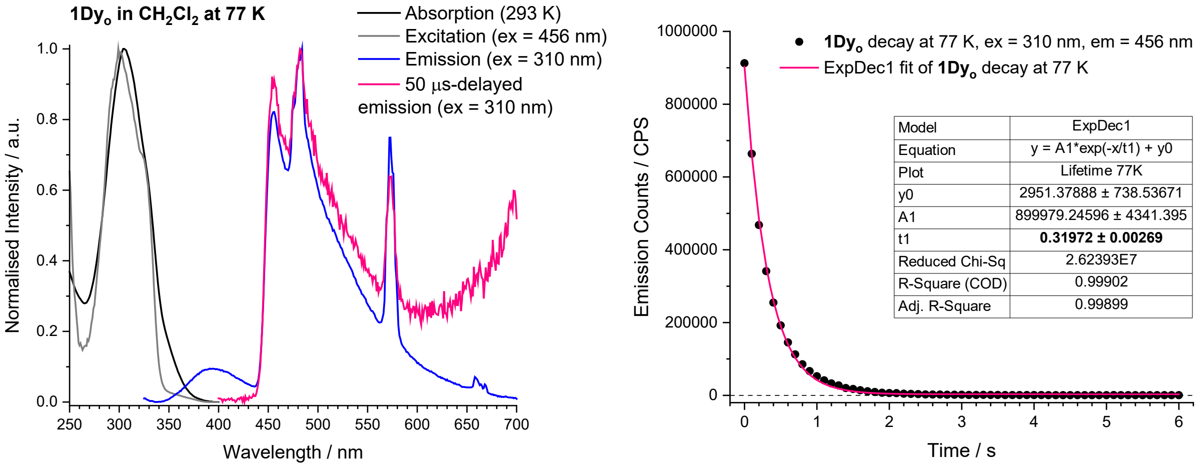

Model	ExpDec1
Equation	y = A1*exp(-x/t1) + y0
Plot	Lifetime 77K
y0	2951.37888 ± 738.53671
A1	899979.24596 ± 4341.395
t1	**0.31972 ± 0.00269**
Reduced Chi-Sq	2.62393E7
R-Square (COD)	0.99902
Adj. R-Square	0.99899

Figure S15. (left) Normalised absorption, excitation (λ_{em} = 456 nm), emission and 50 µs-delayed emission spectra (λ_{ex} = 310 nm), (right) emission decay of triplet phosphorescence for **1Dy$_o$** in dichloromethane at 77 K (λ_{ex} = 310 nm, λ_{em} = 456 nm). C = 7.9 10^{-6} M.

6. Thermal return studies of the photo-stationary state

Time-profiles were obtained on a homemade photokinetic setup according to the following procedure. The samples were irradiated at 305 nm ± 10 nm at a dedicated temperature under continuous stirring (400 rpm). Temperature and stirring were controlled by a Peltier device. The irradiation light (source Xe lamp Zolix instruments, model Sitius 300P) was selected by passing through a monochromator (Zolix instruments, model Omni-λ200i, halfwidth of ±10 nm). The thermal cycloreversion reactions were monitored by recording absorption spectra every 500 ms with a Flame spectrophotometer (Ocean Insights) combined to a DHBAL-2000 D/Hal lamp equipped with an internal synchronized shutter.

The time-profiles were fitted with a linear function of the kind:

(Eq. S1)

$$\boldsymbol{ln(A) = A_0 + k(T) \times t}$$

The constant k calculated at different temperature allows to obtain the frequency factor A and activation energy Ea of the retrocyclisation reaction follows an Arrhenius' law:

(Eq. S2)

$$\boldsymbol{ln(k) = ln\,(A) - \frac{Ea}{RT}\left(\frac{1}{T}\right)}$$

1Eu$_c$

		A (s^{-1})
T(K)	k (s^{-1})	Ea ($kJ.mol^{-1}$)
290,7	1,60.10^{-3}	
293,15	2,06.10^{-3}	2.8.10^{9}
295,7	2,60.10^{-3}	**62.5**
300.65	3,80.10^{-3}	

Table S6: Kinetic parameters extracted from absorption studies. The decay of the closed isomer signal was fitted by a first order law. Arrhenius law fitting provides the frequency factor A and activation energy Ea parameters.

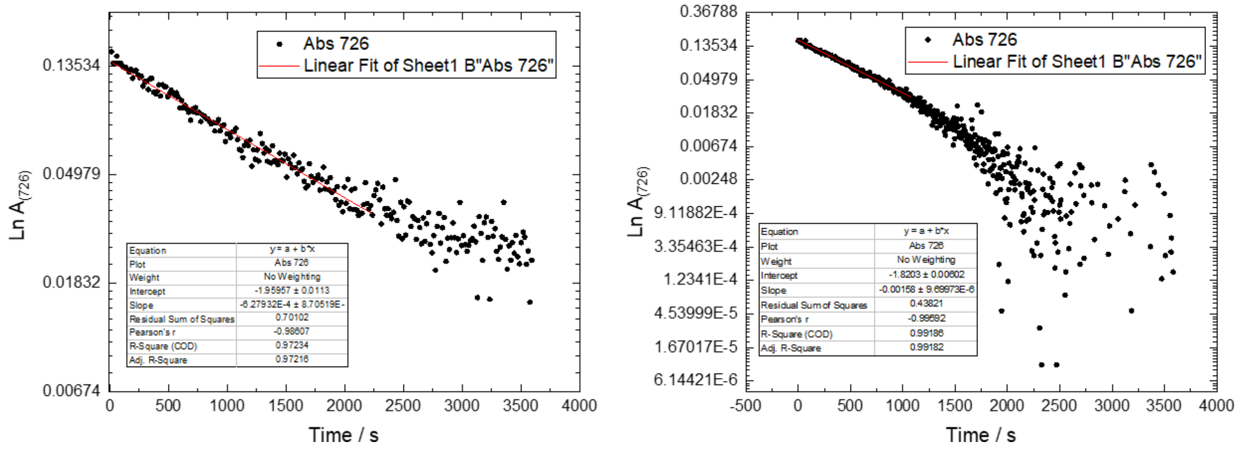

Equation	y = a + b*x
Plot	Abs 726
Weight	No Weighting
Intercept	-1.95957 ± 0.0113
Slope	-6.27932E-4 ± 8.70519E-
Residual Sum of Squares	0.70102
Pearson's r	-0.98607
R-Square (COD)	0.97234
Adj. R-Square	0.97216

Equation	y = a + b*x
Plot	Abs 726
Weight	No Weighting
Intercept	-1.8203 ± 0.00602
Slope	-0.00158 ± 9.69973E-6
Residual Sum of Squares	0.43821
Pearson's r	-0.99592
R-Square (COD)	0.99186
Adj. R-Square	0.99182

Figure S16: Following of the logarithm of the absorbance of **1Eu$_c$** at 726 nm and their first order kinetic linear fit at 15°C (left) and 17.5°C (right), dichloromethane, C = 1.3 10^{-5} M.

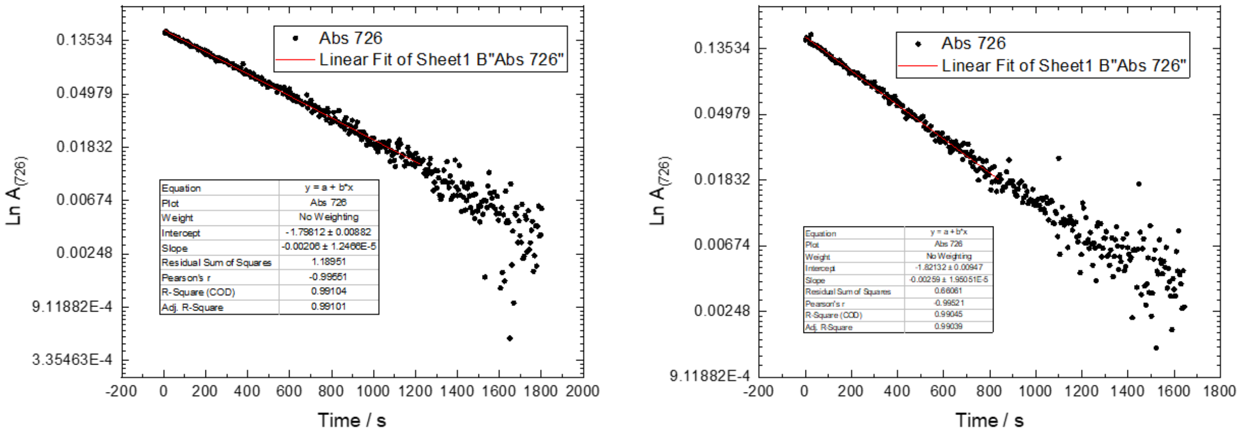

Equation	y = a + b*x
Plot	Abs 726
Weight	No Weighting
Intercept	-1.79812 ± 0.00882
Slope	-0.00206 ± 1.2466E-5
Residual Sum of Squares	1.18951
Pearson's r	-0.99551
R-Square (COD)	0.99104
Adj. R-Square	0.99101

Equation	y = a + b*x
Plot	Abs 726
Weight	No Weighting
Intercept	-1.82132 ± 0.00947
Slope	-0.00259 ± 1.95051E-5
Residual Sum of Squares	0.66061
Pearson's r	-0.99521
R-Square (COD)	0.99045
Adj. R-Square	0.99039

Figure S17: Following of the logarithm of the absorbance of **1Eu$_c$** at 726 nm and their first order kinetic linear fit at 20°C (left) and 22.5°C (right), dichloromethane, C = 1.3 10^{-5} M.

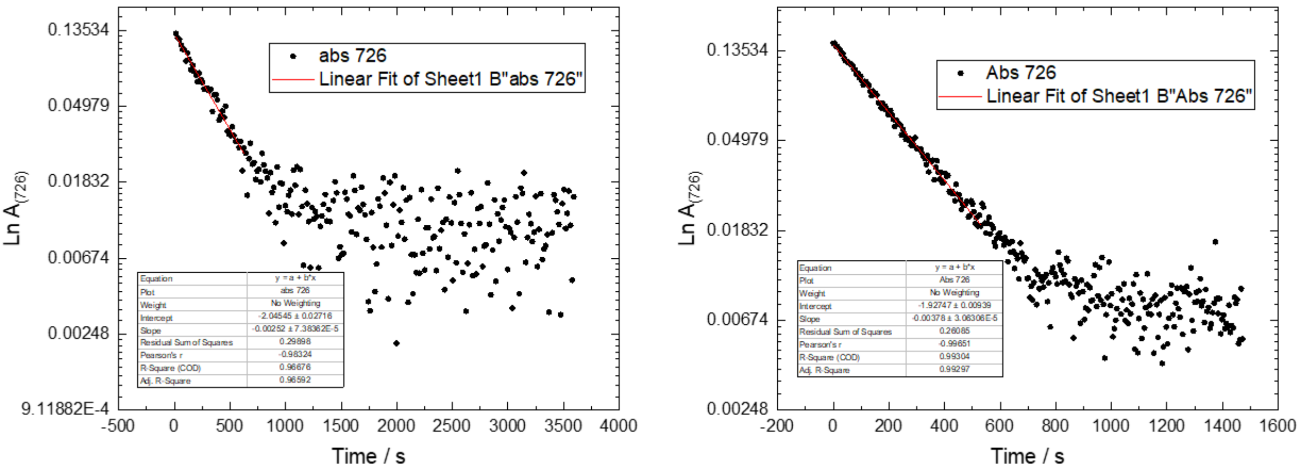

Equation	y = a + b*x
Plot	abs 726
Weight	No Weighting
Intercept	-2.04545 ± 0.02716
Slope	-0.00252 ± 7.38362E-5
Residual Sum of Squares	0.29898
Pearson's r	-0.98324
R-Square (COD)	0.96676
Adj. R-Square	0.96592

Equation	y = a + b*x
Plot	Abs 726
Weight	No Weighting
Intercept	-1.92747 ± 0.00939
Slope	-0.00378 ± 3.06306E-5
Residual Sum of Squares	0.26085
Pearson's r	-0.99651
R-Square (COD)	0.99304
Adj. R-Square	0.99297

Figure S18: Following of the logarithm of the absorbance of **1Eu$_c$** at 726 nm and their first order kinetic linear fit at 25°C (left) and 27.5°C (right), dichloromethane, C = 1.3 10^{-5} M.

7. References

[1] Norel, L.; Bernot, K.; Gendron, F.; Gould, C. A.; Roisnel, T.; Delbaere, S.; Le Guennic, B.; Jacquemin, D.; Rigaut, S., *Chemistry Squared* 2020, ***4***, 2.